Available online at www.sciencedirect.com

SciVerse ScienceDirect

journal homepage: www.elsevier.com/locate/he

Hydrogen production via steam and autothermal reforming of beef tallow: A thermodynamic investigation

Noureddine Hajjaji [a,*], *Marie-Noëlle Pons* [b]

[a] *Unité de Recherche Catalyse et Matériaux pour l'Environnement et les Procédés URCMEP (UR11ES85), Ecole Nationale d'Ingénieurs de Gabès, Université de Gabès, Rue Omar Ibn Alkhattab, 6029 Gabès, Tunisia*

[b] *Laboratoire Réactions et Génie des Procédés – CNRS, Université de Lorraine, 1, rue Grandville, BP 20451, 54001 Nancy cedex, France*

ARTICLE INFO

Article history:
Received 19 September 2012
Received in revised form
19 November 2012
Accepted 25 November 2012
Available online 23 December 2012

Keywords:
Hydrogen
Beef tallow
Autothermal steam reforming
Steam reforming
Thermodynamic analysis
Thermoneutral

ABSTRACT

A thermodynamic analysis of hydrogen production via steam and autothermal reforming of beef tallow has been carried out via the Gibbs free energy minimization method. Equilibrium calculations are performed at atmospheric pressure with a wide range of temperatures (400–1200 °C), steam-to-beef tallow ratios (1–15) and oxygen-to-beef tallow ratios (0.0–2.0).

The results show that the optimum conditions for steam reforming can be achieved at reforming temperatures between 700 °C and 900 °C and a steam-to-beef tallow ratio of approximately 5. Optimal operating conditions of $T = 700$ °C and a steam-to-beef tallow ratio of 5 are proposed. With this condition, a hydrogen yield of 170 moles/kg beef tallow and a CO concentration in the synthesis gas of 4.77% with a trace content of CH_4 (0.01%) can be obtained without coke formation.

The most favorable conditions for hydrogen production from autothermal systems are achieved at the temperature, steam-to-beef tallow ratio and oxygen-to-beef tallow ratio of 600–800 °C, 3–5 and 0.0–0.45, respectively. Thermoneutral conditions can be accomplished with an oxygen-to-beef tallow ratio of 0.384–0.427. The recommended conditions are a steam-to-beef tallow ratio of 5, $T = 600$ °C and an oxygen-to-beef tallow ratio of 0.422. Under these conditions, 150 moles H_2/kg beef tallow can be produced with only 2.92% CO and 0.07% CH_4 in the synthesis gas.

1. Introduction

Recently, concerns regarding carbon dioxide emissions from fossil fuel combustion and their impact on the Earth's climate have been growing, not only among the scientific community but also in the general population. As a consequence, the Kyoto protocol and other international agreements have been signed to secure an international commitment to reduce the global CO_2 emissions [1]. Therefore, efforts for reducing these emissions has led to an increase in research for new technologies, not only for new ways of converting fossil fuels that would allow for CO_2 capture and storage but also for the generation of alternative fuels to replace traditional fuels in thermal engines and boilers, for instance, with lower contributions to greenhouse gas emissions. Due to the increasing interest in replacing fossil fuels, renewable energy sources,

* *Corresponding author*. Tel.: +216 24 04 04 00; fax: +216 75 29 00 41.
E-mail address: hajjaji.nour@gmail.com (N. Hajjaji).

0360-3199/$ – see front matter
http://dx.doi.org/10.1016/j.ijhydene.2012.11.120

such as alternative and non-traditional fuels, are subjects of great interest around the world, although their use is still a challenge in both practical and modeled combustion systems. Renewable energy sources include materials that supply energy without depleting their supply and are considered environmentally friendly when used in thermochemical conversion technologies [2].

Currently, there is great interest in the use of hydrogen as a fuel, especially in high-efficiency systems such as fuel cells, and its application in the transportation sector. With pure hydrogen, a fuel cell vehicle is a true "zero emission" vehicle, producing only water as a by-product. Moreover, hydrogen has the benefit of improving the security of fuel supplies because it can be produced from diverse primary energy sources, such as hydrocarbons, biomass, water, or solar energy [3]. Hydrogen appears, therefore, to be a panacea for the global energy crisis and many environmental problems.

H_2 is, however, an energy carrier, not an energy source. Although it is found naturally in hydrogen-rich compounds, it cannot be extracted in the same way as natural gas or oil; it needs to be recovered by applying energy. Conventional industrial hydrogen production methods, such as the steam reforming of methane and partial oxidation of fossil fuels, are energy intensive and require high temperatures (>850 °C), resulting in the release of carbon dioxide and other greenhouse gases and pollutants as by-products [4]. Under these circumstances, biological hydrogen production from a renewable substrate appears to be a promising way to replace traditional methods, as it can produce hydrogen cheaply under ambient conditions without adding pollution to the environment [5,6]. Consequently, in the last few years, biohydrogen has become a hot topic, which is impressively demonstrated by the large number of investigations published to address this issue.

Current industrial practices have led to the generation of an enormous amount of crude fatty materials as waste, and these materials are difficult to treat and valorize [7]. One such material is tallow from slaughterhouses, food industry and meat industry waste. Like vegetable oils, tallow is a triglyceride (Fig. 1). A triglyceride consists of a three-carbon glycerol head groups (shown in blue) conjugated to three fatty acid chains [8]. All triglycerides have the same basic structure, and the differences in properties and use of commercial triglycerides depends entirely on the length, degree of unsaturation and other chemical modifications to the fatty acid chains [8].

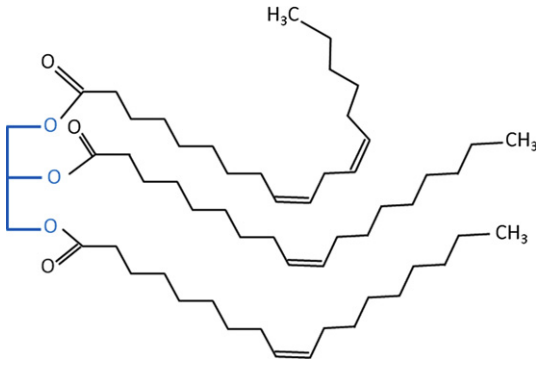

Fig. 1 – Structure of a triglyceride [8].

The main constituents of tallow are fatty acids, including saturated (sum of palmitic, $C_{16:0}$, and stearic, $C_{18:0}$, acid) and unsaturated (sum of oleic, $C_{18:1}$, linoleic, $C_{18:2}$, and linolenic, $C_{18:3}$, acid) acids, and triglycerides [9,10]. C18:0 represents a fatty acid with 18 carbons and no double bonds. C18:1 has 18 carbon atoms and one double bond. These distributions are important because they define the applications for which the oils and fats are most suitable [8].

In the last years considerable attention has been paid to steam and dry reforming studies on synthesis gas production from vegetable oil. Marquevich et al. [11] studied hydrogen production via steam reforming of sunflower oil over Ni/Al catalysts from hydrotalcite materials and compared it with two commercial catalysts for hydrocarbons steam reforming. They concluded that nickel-based catalysts prepared from hydrotalcite precursors are promising catalysts for steam reforming of vegetable oils and may be interesting for producing hydrogen from other biomass-derived feedstocks like fast-pyrolysis oils or ethanol. Dupont et al. [12] investigated a novel process of hydrogen production called unmixed steam reforming (USR) using methane and sunflower oil fuels. They showed that USR process relies on two mass transfer materials which operate on a two-step cycle: an oxygen transfer material (OTM) which provides the heat necessary for the steam reforming reaction, and a CO_2 sorbent which shifts the water gas reaction yielding a hydrogen-rich reformate gas. According to them, the thermal decomposition of the fuel played a significant role in the early hydrogen production concurrent with coking conditions, by causing the OTM to initially reduce. Further investigation of hydrogen production via vegetable oil reforming was reported by Yenumala al. [13]. The authors conducted a thermodynamic equilibrium analysis of steam reforming and autothermal steam reforming of vegetable oils to synthesis gas. The effects of various parameters of reforming reactions on hydrogen yield and selectivity of CO and methane was studied.

Many researchers have reported the use of animal fats, such us beef tallow (BT), as a substrate for the production of biodiesel and glycerin via the transesterification process [14–17]. Biodiesel fuels produced from tallow and vegetable oils have comparable compositions [18]. However, there are some differences; the main one is that the tallow-based biodiesel (TBD) contains more saturated fatty esters [18]. Tallow as a biodiesel feedstock has some advantages and disadvantages. TBD has a higher cetane number than plant oil biodiesel, which means that TBD is cleaner and burns more efficiently in diesel engines [8]. However, tallow biodiesel has a higher cloud point because of the high levels of saturated fatty acids. Its higher cloud point means that tallow biodiesel tends to crystallize out at low temperatures, creating problems in engines. Used pure (100%) tallow biodiesel would not meet the European standards. However, when blended at 5% into conventional diesel, the mixture meets the relevant fuel quality standards [19].

With increased production of cattle, especially in India and China, an excess of tallow is expected to appear on the world market. The total world production of cattle carcasses is annually estimated at 57 million tons and contains 10% fat [20,21]. Therefore, it is essential to find useful applications for renewable and cheap tallow. We believe that tallow is

a promising feedstock for producing hydrogen because the oxygen content is low and the potential yield of hydrogen is high. Moreover, tallow is a promising alternative for renewable hydrogen production due to the highly centralized generation in slaughter processing facilities and historically low prices; this may have energy, environmental, and economic advantages that could be exploited. Hydrogen obtained from tallow has been proposed to be a low-risk end use for tallow from livestock that are removed from the food chain [22,23]. However, the thermodynamic equilibrium investigation of tallow has not been considered in the past because of its complex chemical structure and the unavailability of physical and chemical properties. Thermodynamic equilibrium investigation is an important tool to obtain equilibrium products composition and identify thermodynamically favorable operating conditions of the process. It is an aid in reactor modeling, in examining kinetic schemes or reaction mechanisms, and in identifying rate-controlling processes [24].

This paper intends to identify thermodynamically favorable operating conditions at which beef tallow may be converted to hydrogen via the steam reforming (SR) and autothermal reforming (ATR) processes. The synthesis gas composition was determined by simulations to minimize the Gibbs free energy using the Aspen Plus™ 10.2 software (Aspen Technology, Inc., Burlington, MA, USA).

2. Modeling and simulation methodology

2.1. Beef tallow characterization

Table 1 gives the typical fatty acid composition of the beef tallow considered in this work.

For simplicity of analysis, the beef tallow is considered as a mixture of triglycerides with the same three fatty acid groups in their backbone. Moreover, trimyristin, tripalmitin, tristearin, tripalmitoleic, trioleate, trilinolein and trilinolenic are not included in the Aspen Plus™ databank; they needed to be added before the simulation could be started. This operation required various data, such as the chemical structure, normal boiling point, molecular weight, temperature-dependent vapor pressures and heat capacity, standard enthalpy and Gibbs free energy of formation of these compounds, to be inserted into the Aspen Plus™ dialog box [26].

Considering the low level of some triglycerides and the difficulty to achieve all required regression data, the study presented here ignores compounds having a composition less than 5%. The beef tallow is assumed to be, in weight percent, 30% tripalmitin, 20% tristearin and 50% trioleate. Main components and average molecular composition of beef tallow are depicted in Table 2.

All required data for regression of property method were obtained from different literature sources [13,27,28] and were given in Table 3.

2.2. Minimization of the Gibbs free energy

Equilibrium compositions were calculated by minimizing the Gibbs free energy within the environment of Aspen Plus™. The R-Gibbs reactor [26] has been selected for the calculations using the UNIF-LBY equation of state.

Gibbs free energy is the most commonly used function to identify the equilibrium state. For a system with multiple species and phases, equilibrium calculations can be performed through the Gibbs-energy minimization method.

The total Gibbs free energy (G^t) of a system is given by Eq. (1)

$$G^t = \sum_{i=1}^{N} n_i \overline{G_i} = \sum_{i=1}^{N} n_i \mu_i = \sum_{i=1}^{N} n_i G_i^0 + RT \sum_{i=1}^{N} n_i \ln \frac{f_i}{f_i^0} \quad (1)$$

where $\overline{G_i}$ is the partial molar Gibbs free energy of species i, G_i^0 is the standard Gibbs free energy, μ_i is the chemical potential, R is the molar gas constant, T is the temperature of system, P is the pressure of system, f_i is the fugacity in system, f_i^0 is the standard-state fugacity and n_i is the moles of species i.

For reaction equilibrium in the gas phase $f_i = y_i \overline{\varphi_i} P, f_i^0 = P^0$ and $G_i^0 = \Delta G_{fi}^0$

The minimum Gibbs free energy of each gaseous species and that of the total system can be expressed by Eqs. (2) and (3) respectively, with the Lagrange's undetermined multiplier method.

$$\Delta G_{fi}^0 + RT \ln \frac{y_i \overline{\varphi_i} P}{P^0} + \sum_k \lambda_k a_{ik} = 0 \quad (2)$$

$$\sum_{i=1}^{N} n_i \left(\Delta G_{fi}^0 + RT \ln \frac{y_i \overline{\varphi_i} P}{P^0} + \sum_k \lambda_k a_{ik} \right) = 0 \quad (3)$$

where P^0 is the standard-state pressure of 101.3 kPa, ΔG_{fi}^0 is the standard Gibbs function of formation of species i, y_i is the gas phase mole fraction, $\overline{\varphi_i}$ is the fugacity coefficient of species i, a_{ik} is the number of atoms of the kth element present in each molecule of species i, λ_k is the Lagrange multiplier and A_k is the total mass of kth element in the feed.

With the constraint of the element balance equation:

$$\sum_{i=1}^{N} n_i a_{ik} = 0 \quad (4)$$

When solid carbon (graphite) is involved in the system, exploitation of the vapor–solid phase equilibrium is applied to the Gibbs-energy of carbon as shown in Eq. (5). Substituting Eq. (1) by Eq. (2) for gaseous species and by Eq. (5) for solid species gives the minimization function of Gibbs-energy as shown in Eq. (6):

Table 1 – Typical fatty acid composition of beef tallow (% weight) [25].

Saturated			Unsaturated				Others
Myristic 14:0	Palmitic 16:0	Stearic 18:0	Palmitoleic 16:1	Oleic 18:1	Linoleic 18:2	Linolenic 18:3	
3	26	14	3	47	3	1	3

Table 2 – Main components and average molecular composition of beef tallow.

	Tripalmitin	Tristearin	Trioleate
Formula	$C_{51}H_{98}O_6$	$C_{57}H_{110}O_6$	$C_{57}H_{104}O_6$
Molecular weight	807.32	891.47	885.43
Composition (% w)	30	20	50
Composition (% mol)	32.02	19.33	48.65
Average molecular composition	$C_{55.08}H_{103.24}O_6$		

$$\overline{G}_{C(g)} = \overline{G}_{C(s)} = G_{C(s)} \cong \Delta G^0_{fC(s)} = 0 \quad (5)$$

$$\sum_{i=1}^{N} n_i \left(\Delta G^0_{fi} + RT \ln \frac{y_i \overline{\varphi_i} P}{P^0} + \sum_k \lambda_k a_{ik} \right) + \left(n_c \Delta G^0_{fC(s)} \right) = 0 \quad (6)$$

where $\overline{G}_{C(s)}$, $\overline{G}_{C(g)}$, $G_{C(s)}$, $\Delta G^0_{fC(s)}$ and n_c are the partial molar Gibbs free energy of solid carbon, the partial molar Gibbs free energy of gaseous carbon, the molar Gibbs free energy of solid carbon, the standard Gibbs free energy of formation of solid carbon, and moles of carbon, respectively.

The primary species involved in BT reforming are CO_2, H_2O, CO, H_2, CH_4, $C_{(graphite)}$, tripalmitin ($C_{51}H_{98}O_6$), tristearin ($C_{57}H_{110}O_6$), trioleate ($C_{57}H_{104}O_6$), ethylene (C_2H_4), ethane (C_2H_6), propylene (C_3H_6), propane (C_3H_8), n-butane (C_4H_{10}), isobutane (C_4H_{10}), 1-butene (C_4H_8), 2-cis-butene (C_4H_8), 2-trans-butene (C_4H_8), isobutylene (C_4H_8), methanol (CH_4O),formaldehyde (CH_2O), ethanol (C_2H_6O), methanol (CH_4O), formaldehyde (CH_2O), acetaldehyde (C_2H_4O), acetic acid ($C_2H_4O_2$), acetone (C_3H_6O), glycerol ($C_3H_8O_3$), acrolein (C_3H_4O), *n*-butanol ($C_4H_{10}O$), methyl ethyl ketone, and allyl alcohol (C_3H_6O).

3. Hydrogen production by beef tallow reforming

3.1. *Steam reforming (SR)*

SR is an endothermic reaction in which the substrate is treated with steam in the presence of a catalyst to produce synthesis gas (SG). The steam reforming of an oxygenated hydrocarbon, such BT, involves a complex reaction system, with undesired reaction paths [29].

The key reactions concerned in the reforming process are as follows.

$$C_{55.08}H_{103.24}O_6 + 49.08H_2O \leftrightarrow 55.08CO + 100.7H_2 \quad \Delta H^\circ_{298\ K} = 10.07\ MJ/mol \quad (7)$$

Water gas shift (WGS):

$$CO + H_2O \leftrightarrow CO_2 + H_2 \quad \Delta H^\circ_{298\ K} = -41.17\ kJ/mol \quad (8)$$

Methanation:

$$CO + 3H_2 \leftrightarrow CH_4 + H_2O \quad \Delta H^\circ_{298\ K} = -206.11\ kJ/mol \quad (9)$$

$$CO_2 + 4H_2 \leftrightarrow CH_4 + 2H_2O \quad \Delta H^\circ_{298\ K} = -164.94\ kJ/mol \quad (10)$$

Methane CO_2 reforming:

$$CO_2 + CH_4 \leftrightarrow 2H_2 + 2CO \quad \Delta H^\circ_{298\ K} = 247.28\ kJ/mol \quad (11)$$

Carbon formation:

$$2CO \leftrightarrow CO_2 + C \quad \Delta H^\circ_{298\ K} = -172.43\ kJ/mol \quad (12)$$

$$CH_4 \leftrightarrow 2H_2 + C \quad \Delta H^\circ_{298\ K} = 74.85\ kJ/mol \quad (13)$$

$$CO + H_2 \leftrightarrow C + H_2O \quad \Delta H^\circ_{298\ K} = -131.26\ kJ/mol \quad (14)$$

$$C_{55.08}H_{103.24}O_6 + 104.16H_2O \leftrightarrow 55.08CO_2 + 155.78H_2 \quad \Delta H^\circ_{298\ K} = 7.80\ MJ/mol \quad (15)$$

This overall reaction (Eq. (15)) is endothermic and requires a large amount of external heat. The equilibrium composition of the SG depends on the reformer temperature (T) and pressure (P), as well as the initial composition of the BT steam mixture expressed by the steam to carbon molar ratio (S/C).

The S/C ratio is given by Eq. (16) [13].

Table 3 – Properties of tristearin, tripalmitin, and trioleate [13,27,28].

		Tripalmitin	Tristearin	Trioleate
Normal boiling point, K		1086	1033	1120
Density, kg/m^3		916	909	911.36
Standard heat of formation, MJ/mole		−2.05	−2.18	−1.84
Standard Gibbs free energy, kJ/mole		−555.0	−504.5	−263.8
Temperature-dependent heat capacity	T, K	Heat capacity, J/g K		
	353	2.1142	2.1790	1.7053
	373	2.1624	2.2272	1.7812
	393	2.2115	2.2763	1.8549
	413	2.2612	2.3260	1.9266
	433	2.3114	2.3762	1.9963
	453	2.3618	2.4266	2.0639
Temperature-dependent vapor pressure	P, mm Hg	T, °C		
	0.05	571.0	586.0	585.8
	0.001	512.0	526.0	537.7

$$\text{Steam}-\text{to}-\text{carbon ratio} = \left(\frac{\text{moles of steam}}{\text{moles of BT}}\right) \Big/ \left(\frac{\text{moles of steam}}{\text{moles of BT}}\right)_{\text{stoichiometric}} = \frac{(\text{moles of steam})}{104.16 \times (\text{moles of BT})} \quad (16)$$

This investigation was performed at atmospheric pressure because previous investigations of SR of oxygenated hydrocarbons have already shown that higher pressures are thermodynamically unfavorable [30,31]. The increase in pressure shifts the equilibrium towards the reactants in the overall hydrogen forming reactions (Eq. (15)). Carbon monoxide methanation increases with an increase in pressure, which results in increased methane selectivity and negatively affects the hydrogen and carbon monoxide yields [32].

3.2. Autothermal reforming (ATR)

Autothermal reforming has been suggested to ameliorate the difficulties of steam reforming. Specifically, autothermal reformation overcomes the steam reformation limitations of high temperature operations and fast dynamic responses. Additionally, an autothermal reformer can reduce the size, weight, start-up, shut-down, and other dynamic response times [33,34]. Autothermal reforming combines POX and SR in a single process. The POX reaction is exothermic (i.e., it produces heat), while a SR reaction is endothermic, and heat must be generated externally for the reforming process. Typically, ATR reactions are considered to be thermally self-sustaining and consequently do not produce or consume external thermal energy. The main chemical reaction for POX of BT is given by Eq. (17).

$$C_{55.08}H_{103.24}O_6 + 24.54O_2 \leftrightarrow 55.08CO + 51.62H_2 \quad \Delta H^{\circ}_{298\ K} = -3.95\ \text{MJ/mol} \quad (17)$$

The overall reaction of ATR can be expressed as Eq. (18), a combination of SR and POX.

$$C_{55.08}H_{103.24}O_6 + aO_2 + bH_2O \leftrightarrow cCO + dCO_2 + eH_2 + fCH_4 + gC \quad (18)$$

The stoichiometric coefficients (a–g) depend on the reformer temperature (T), pressure (P), (S/C) ratio and the oxygen to carbon molar ratio (O/C).

The O/C ratio is given by Eq. (19) [13].

$$\text{Oxygen}-\text{to}-\text{carbon ratio} = \left(\frac{\text{moles of oxygen}}{\text{moles of BT}}\right) \Big/ \left(\frac{\text{moles of oxygen}}{\text{moles of BT}}\right)_{\text{stoichiometric}} = \frac{(\text{moles of oxygen})}{24.54 \times (\text{moles of BT})} \quad (19)$$

The oxygen source can be either pure oxygen or air. In the present work, pure oxygen was considered for thermodynamic equilibrium investigation since using air as oxygen-carrier increases the nitrogen-content in the reformer effluent strongly. However it would an interesting issue to determine whether using air instead of pure oxygen could improve hydrogen production. It is well known that pure oxygen increases significantly production costs.

4. Results and discussion

4.1. Beef tallow: thermodynamically possible products

BT reforming involves a complex reaction system with undesired reaction paths. Main reforming products are H_2, CH_4, CO_2, CO and H_2O. Depending on the catalyst employed and the completeness of conversion, the product distributions in the synthesis gas may be different than described above. In this paper, equilibrium compositions were calculated by the minimization of the Gibbs free energy with the aid of the Aspen Plus™ software. This code requires identification of the possible products that might be generated as intermediates or products from side reactions [26]. Therefore, the standard product set was expanded to include these possible products. The expanded product set is given in Table 4.

Table 4 shows that triglycerides are fully converted and the concentrations of ethane, ethylene, acetylene and other oxygenated compounds in the product stream can be considered as thermodynamically unstable products and are therefore negligible. These compounds are formed by thermal cracking and are also converted through SR reaction. However, their possible occurrence in experimental work is because the reforming reactions are in practice under kinetic control [29].

Therefore, the component list for further thermodynamic equilibrium analysis is restricted to CO, CO_2, H_2, CH_4, H_2O and $C_{(graphite)}$.

4.2. Coke formation

Coke formation during the catalytic steam reforming could lead to the deactivation of catalysts, resulting in low durability and activity [35,36]. Operating the reforming system (SR and ATR) under the coke-free regions could avoid coke formation. Coke formation was, consequently, investigated to determine the coke-formed and coke-free regions.

Fig. 2 illustrates the coke formation (kg C/kg BT) as a function of reforming temperature for different S/C operating conditions. There is a great potential for coke formation for an S/C ratio of 0.25, for all reforming temperatures investigated. At a given temperature, an increase in the S/C lowered the amount of coke formed; for S/C ratios higher than 1, no coke

Table 4 – Synthesis gas composition (% mol) and moles C (graphite)/ mole BT in feed for different S/C ratio, T = 500 °C and P = 1 atm.

Species	SR			ATR[a]		
	S/C = 0.25	S/C = 1	S/C = 3	S/C = 0.25	S/C = 1	S/C = 3
H_2O	2.26	36.11	59.34	34.14	44.29	76.45
CO_2	17.44	15.64	10.10	12.79	19.92	12.76
CO	14.31	2.44	0.88	2.24	2.19	0.34
H_2	9.54	28.97	26.75	30.82	25.20	10.39
CH_4	56.45	16.84	2.93	20.00	8.40	0.05
C	2.63	–	–	29.19	–	–
Tripalmitin	3.43×10^{-37}	7.26×10^{-39}	2.13×10^{-43}	7.19×10^{-41}	1.13×10^{-43}	8.17×10^{-43}
Tristearin	1.27×10^{-38}	3.14×10^{-40}	8.23×10^{-41}	4.22×10^{-39}	3.19×10^{-44}	4.11×10^{-45}
Trioleate	7.66×10^{-38}	9.42×10^{-40}	9.65×10^{-42}	6.47×10^{-39}	4.14×10^{-45}	5.73×10^{-46}
Ethylene (C_2H_4)	1.16×10^{-4}	1.12×10^{-6}	3.95×10^{-8}	9.83×10^{-7}	3.55×10^{-7}	7.80×10^{-11}
Ethane (C_2H_6)	4.69×10^{-3}	1.37×10^{-4}	4.50×10^{-6}	1.30×10^{-4}	3.89×10^{-5}	3.41×10^{-9}
Propylene (C_3H_6)	7.07×10^{-7}	6.70×10^{-10}	4.47×10^{-12}	6.56×10^{-10}	1.21×10^{-10}	3.89×10^{-16}
Propane (C_3H_8)	2.23×10^{-6}	6.41×10^{-9}	3.95×10^{-11}	6.75×10^{-9}	1.03×10^{-9}	1.32×10^{-15}
n-Butane (C_4H_{10})	1.01×10^{-9}	2.86×10^{-13}	3.32×10^{-16}	3.35×10^{-13}	2.61×10^{-14}	–
Isobutane (C_4H_{10})	6.97×10^{-10}	1.97×10^{-13}	2.28×10^{-16}	2.30×10^{-13}	1.80×10^{-14}	–
1-Butene (C_4H_8)	3.04×10^{-10}	2.82×10^{-14}	3.54×10^{-17}	3.08×10^{-14}	2.90×10^{-15}	1.37×10^{-22}
2-Cis-butene (C_4H_8)	3.21×10^{-10}	2.99×10^{-14}	3.75×10^{-17}	3.26×10^{-14}	3.07×10^{-15}	1.45×10^{-22}
2-Trans-butene (C_4H_8)	4.04×10^{-10}	3.76×10^{-14}	4.71×10^{-17}	4.10×10^{-14}	3.87×10^{-15}	1.82×10^{-22}
Isobutylene (C_4H_8)	7.18×10^{-10}	6.69×10^{-14}	8.39×10^{-17}	7.29×10^{-14}	6.89×10^{-15}	3.23×10^{-22}
Methanol (CH_4O)	1.57×10^{-7}	2.47×10^{-7}	7.63×10^{-8}	7.29×10^{-14}	6.89×10^{-15}	3.23×10^{-22}
Formaldehyde (CH_2O)	9.38×10^{-7}	4.85×10^{-7}	1.63×10^{-7}	1.85×10^{-07}	1.70×10^{-7}	4.37×10^{-9}
Ethanol (C_2H_6O)	5.78×10^{-10}	8.91×10^{-11}	5.19×10^{-12}	3.40×10^{-7}	3.79×10^{-7}	2.41×10^{-8}
Methanol (CH_4O)	1.57×10^{-7}	2.47×10^{-7}	7.63×10^{-8}	7.29×10^{-14}	6.89×10^{-15}	3.23×10^{-22}
Formaldehyde (CH_2O)	9.38×10^{-7}	4.85×10^{-7}	1.63×10^{-7}	1.85×10^{-07}	1.70×10^{-7}	4.37×10^{-9}
Acetaldehyde (C_2H_4O)	2.20×10^{-7}	1.12×10^{-8}	7.04×10^{-10}	7.45×10^{-11}	3.50×10^{-11}	1.31×10^{-14}
Acetic acid ($C_2H_4O_2$)	2.79×10^{-8}	7.48×10^{-9}	8.39×10^{-10}	8.72×10^{-9}	4.98×10^{-9}	4.61×10^{-12}
Acetone (C_3H_6O)	2.38×10^{-9}	1.19×10^{-11}	1.41×10^{-13}	5.19×10^{-9}	4.72×10^{-9}	1.82×10^{-11}
Glycerol ($C_3H_8O_3$)	1.16×10^{-26}	4.88×10^{-27}	1.69×10^{-28}	1.03×10^{-11}	3.02×10^{-12}	4.07×10^{-17}
Acrolein (C_3H_4O)	4.72×10^{-10}	7.76×10^{-13}	9.97×10^{-15}	-	2.11×10^{-27}	–
n-Butanol ($C_4H_{10}O$)	7.74×10^{-17}	1.04×10^{-19}	2.38×10^{-22}	1.28×10^{-14}	3.09×10^{-15}	1.69×10^{-20}
Methyl ethyl ketone	1.38×10^{-21}	6.77×10^{-25}	1.51×10^{-27}	1.20×10^{-19}	1.47×10^{-20}	–
Allyl alcohol (C_3H_6O)	8.02×10^{-15}	4.00×10^{-17}	4.75×10^{-19}	6.28×10^{-13}	2.22×10^{-13}	7.51×10^{-18}

a O/C ratio is adjusted to obtain reactor temperature of 500 °C at adiabatic condition.

can be formed at temperatures above 300 °C. Otherwise, at low S/C ratios, coke formation plot does not show a monotone behavior but two regions with strong coke formation. This can be explained by the competition between the different coke formation reactions (Eqs. (12)–(14)). In fact, these reactions are in equilibrium and the formation of coke via exothermic reactions (Eqs. (12)–(14)) becomes less favored as the temperature increases whereas coke formation via endothermic reaction (Eq. (13)) becomes increasingly important at

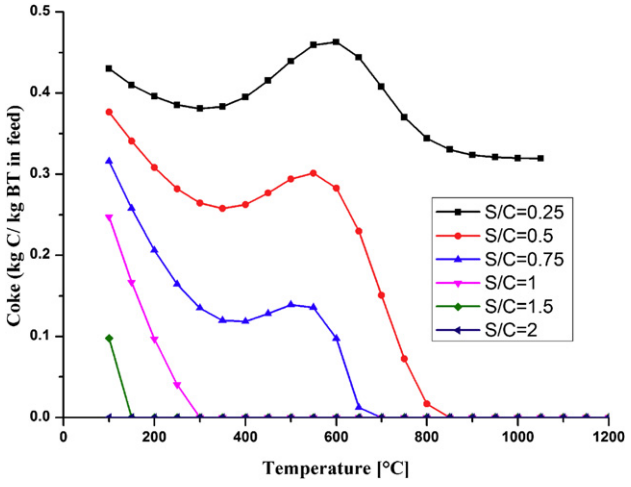

Fig. 2 – Thermodynamically predicted coke formation of SR of BT as function of temperature for different S/C ratio at 1 atm.

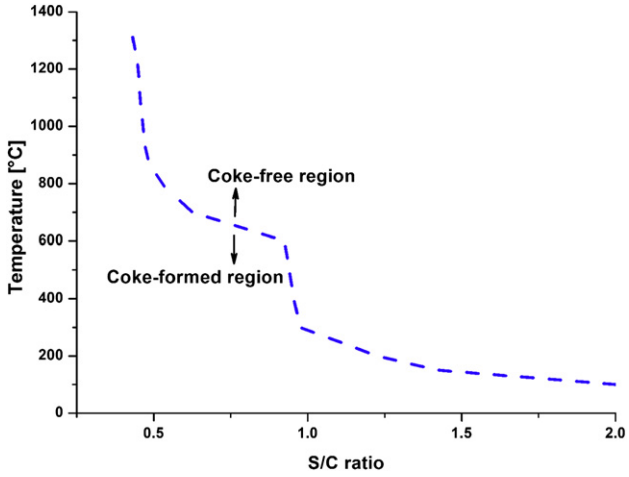

Fig. 3 – Coke formation boundary of SR of BT as a function of S/C ratio and temperature at 1 atm.

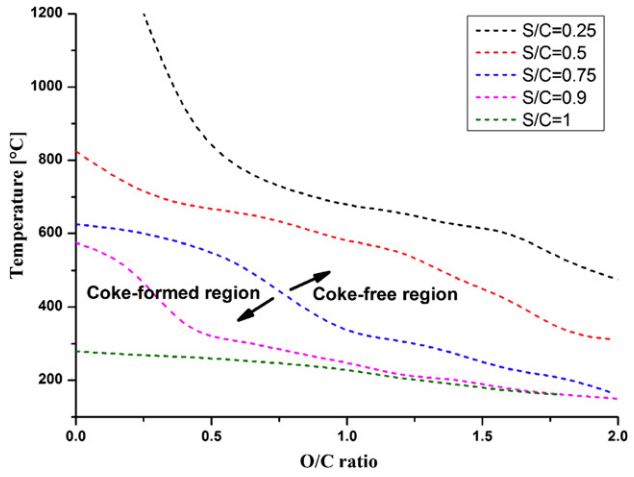

Fig. 4 – Coke formation boundary of ATR of BT as a function of O/C ratio for different S/C ratio at 1 atm.

higher temperature. Therefore, the peak of coking formation (at about 550 °C), shown in Fig. 2, is a result of the competition between carbon deposition and carbon elimination in the whole temperature range.

For a given S/C ratio, the temperature at which the first disappearance of carbon solid (T_{CD}) was achieved, was considered to be the carbon boundary. The regions above and below the boundary are the coke-free and coke-formed regions, respectively. Fig. 3 shows that the coke formation is avoided by increasing the reactor temperature and/or the S/C ratio. The competition between the different coke formation reactions, described above, causes the peak of coking formation (at about 550 °C) and makes the coke-formed region wide at temperature around 550 °C (Fig. 3).

The coke formation behavior in the case of ATR has been evaluated. Fig. 4 shows the temperature of the coke formation boundary for different S/C ratios over different O/C ratios.

For a given temperature, coke formation is suppressed by the increase of the O/C ratio and/or the increase of the S/C ratio. Moreover, high temperatures and a high S/C ratio inhibit

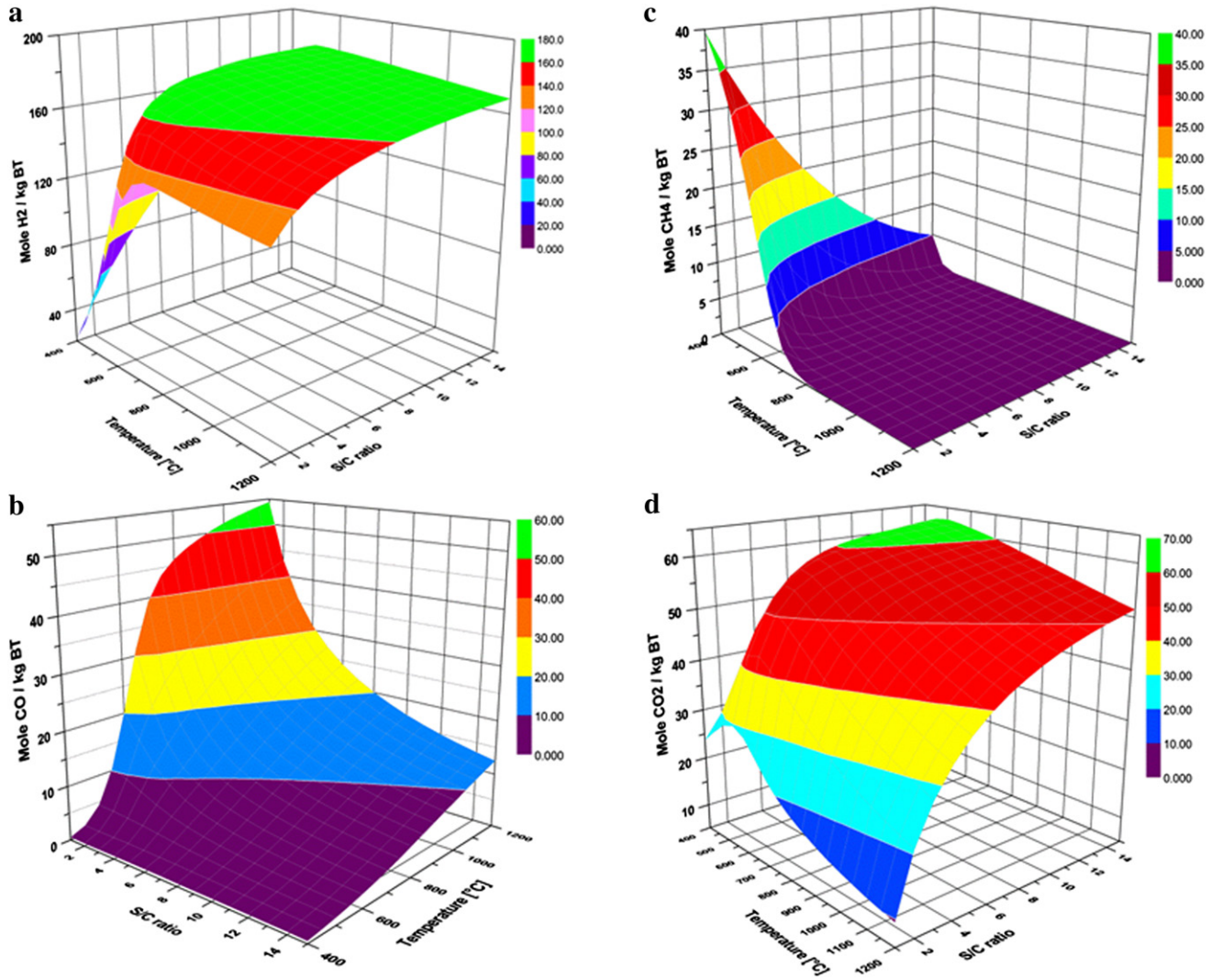

Fig. 5 – Equilibrium synthesis gas yields in BT steam reforming reactor as a function of temperature and S/C ratio at 1 atm (a) H_2 (b) CO (c) CH_4 and (d) CO_2.

Table 5 – Characteristics of BT steam reforming reactor at optimum condition.

Reactor conditions			Synthesis gas composition % (dry basis)			
S/C	T (°C)	P (atm)	H_2	CO	CO_2	CH_4
5	700	1	72.62	4.77	22.59	0.01
Hydrogen productivity			170 mole/kg BT			

coke formation. As an example, avoidance of coke formation is possible for S/C ratios higher than 1 and with temperatures above 300 °C.

4.3. *Beef tallow steam reforming*

The influences of the S/C ratio and the reforming temperature on the equilibrium products of steam reforming of BT are shown in Fig. 5a–d.

Fig. 5a shows the amount of hydrogen produced (moles H_2/kg BT) as a function of the S/C ratio and temperature. The amount of hydrogen produced at temperatures below 500 °C is relatively low compared to that at 700 °C. The hydrogen yield increases with increasing temperature, reaches a maximum, and then decreases slightly. This behavior is the result of inhibition of the exothermic WGS and methanation reactions. Thus, the SR (Eq. (15)) reaction is endothermic and the equilibrium shifts towards the product side with increasing temperature, resulting in increased hydrogen yield. The WGS (Eq. (8)) and methanation (Eqs. (9) and (10)) reactions are exothermic, and the equilibrium shifts towards the reactant side (consumption of hydrogen) with increasing temperature.

Fig. 5b and c show that at low temperatures, methane and carbon dioxide are the most prevalent products with almost no carbon monoxide. At higher temperatures ($T > 800$ °C), the carbon monoxide content strongly increases, which can be attributed to the thermodynamics of the WGS (Eq. (8)) reaction, whereas the methane content is lower. Aiming, simultaneously, for a high H_2 content and a low CO content is a contradiction because the reforming temperature has to be high enough to obtain a reasonable H_2 concentration, whereas the reforming temperature has to be as low as possible to

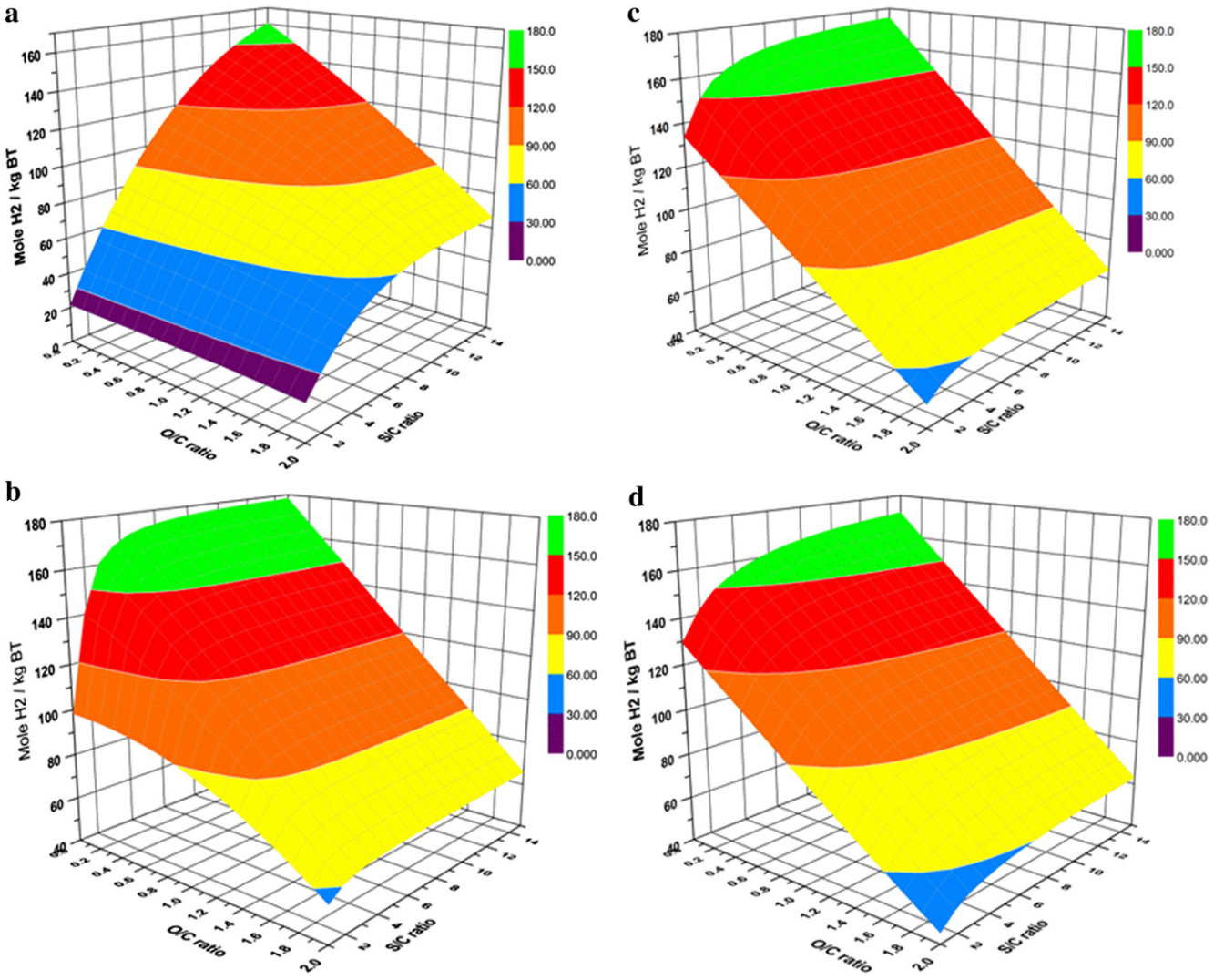

Fig. 6 – Moles of H_2 produced per kg of BT in ATR reactor as function of S/C and O/C ratios at different temperatures and 1 atm: (a) 400 °C, (b) 600 °C, (c) 800 °C and (d) 1000 °C.

minimize the CO content. Taking into account all of the aforementioned considerations, reforming temperatures ranging from 800 °C to 900 °C appear to be reasonable for preeminent BT steam reforming.

The H_2 productivity increases as the S/C ratio increases from 1 to 15 (Fig. 5a). This behavior is consistent with Le Chatelier's Principle, which states that if a dynamic equilibrium is disturbed by changing the operating conditions, the position of equilibrium shifts to counteract the change. With an increase in S/C, the number of moles of water on the reactant side of Eqs. (7) and (8) increases, and hence the equilibrium of SR and water gas shift reaction (WGS) shifts towards the products side, resulting in increased hydrogen yield. The gain in hydrogen productivity is not significant for values of the S/C ratio above 5, whereas the reaction system consumes excessive amounts of water.

As observed from the Fig. 5b, the CO content decreases slightly with an increasing S/C ratio because of an increase in the WGS reaction with S/C. For hydrogen production, it is apparent that CH_4 is not a desirable product because the formation of CH_4 competes with H_2 production. Fortunately, at a given temperature, the methane content decreases as the S/C ratio increases. This effect is mostly appreciable at low temperatures due to the endothermic aspect of methane reforming reaction, which is favored by increasing S/C ratios.

In conclusion, for steam reforming of BT, favorable operating conditions can be ensured by the proper combination of reactor temperature and S/C ratio. The synthesis gas composition that maximizes hydrogen production while minimizing the methane and carbon monoxide contents and without forming coke can be achieved at reforming temperatures between 700 °C and 900 °C and an S/C ratio of approximately 5. Table 5 gives the synthesis gas composition at the optimum conditions for a BT steam reforming reactor.

Under thermodynamic optimum conditions, a hydrogen yield of 170 moles/kg beef tallow can be obtained without coke formation, which appears to be an attractive value for stimulating experimental research. For S/C = 5, about 10.9 kg of steam is required to achieve the reforming reaction of 1 kg of BT. In an entire beef tallow-to-hydrogen plant with heater,

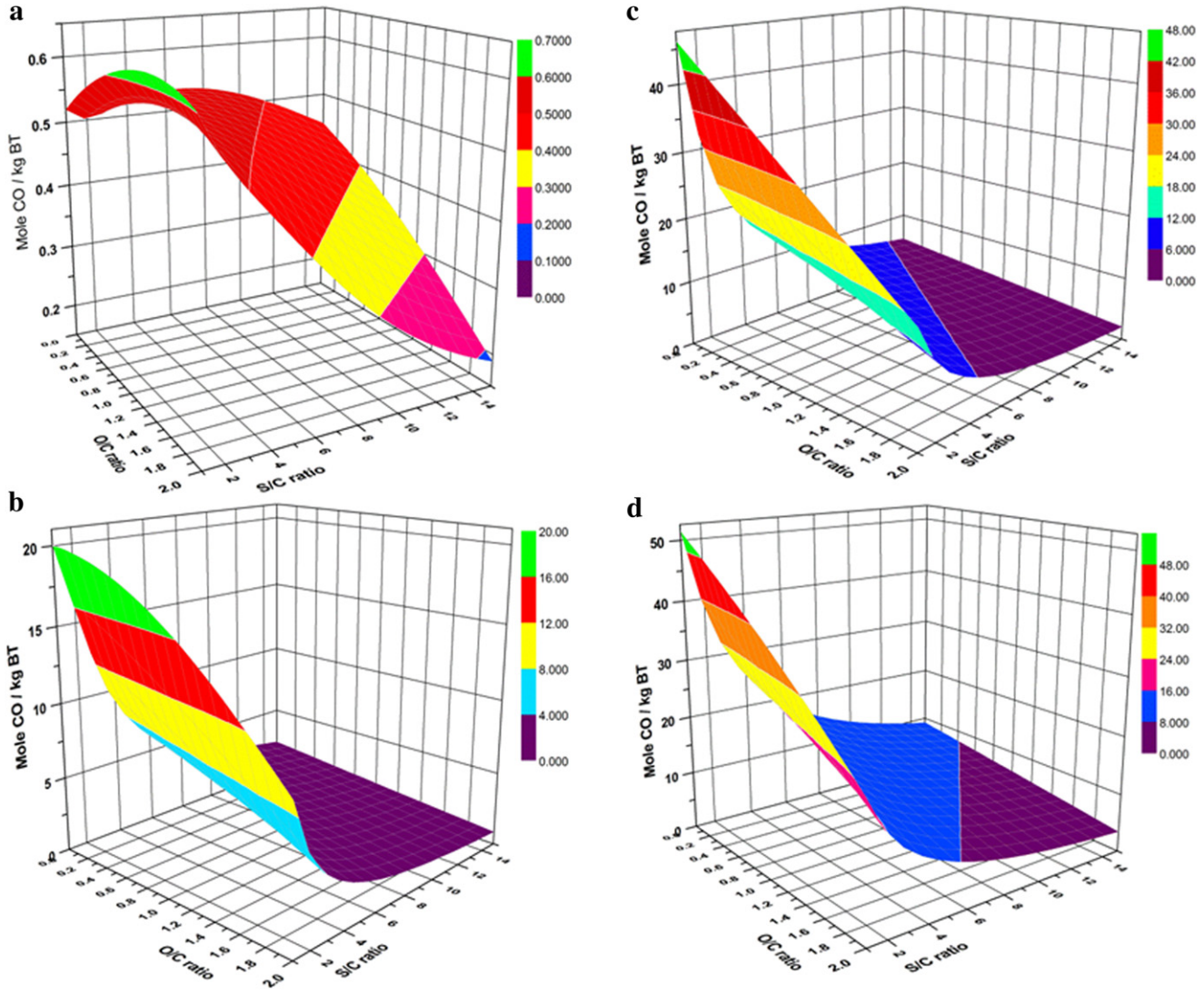

Fig. 7 – Moles of CO produced per kg of BT in ATR reactor as function of S/C and O/C ratios at different temperatures and 1 atm: (a) 400 °C, (b) 600 °C, (c) 800 °C and (d) 1000 °C.

steam generators, etc, the overall energy balance could be very endothermic. Therefore, the energy balance should be established to compute the energy consumption and then the energetic performance of such process.

4.4. *Beef tallow autothermal reforming*

The results of BT autothermal reforming are depicted in Figs. 6–8. The interpretations of the results of the ATR system are, in great part, similar to those of the SR system. In general, as illustrated in Fig. 6, the capacity of hydrogen production is improved at low O/C ratios, especially at high temperatures and S/C ratios. This observation is in good agreement with the ATR of methane [37,38], propane [39,40], ethanol [41,42], glycerol [43,44] and vegetable oil [13].

At a given temperature, an increase in the O/C ratio decreases hydrogen productivity. In fact, the additional oxygen shifts the incomplete oxidation of the synthesis gas to a combustion reaction, resulting in decreased hydrogen yield. Moreover, the increase of the S/C improves the hydrogen production. The gain in hydrogen productivity is not significant for S/C ratios above 5.

As observed in Fig. 7, at low temperatures, the CO content is quite low and increases with increasing temperature. This is because the low temperature favors the exothermic WGS and methanation reactions, leading to a low CO content. As mentioned in the SR system, obtaining a high hydrogen content and a low carbon monoxide content is a contradiction. However, because the amount of hydrogen production can be reduced at low temperatures, moderately high temperatures are preferred, even though a small amount of CO will be produced.

At a given temperature, when the amount of oxygen in the feed is increased, the CO produced at low S/C values becomes more important than the CO produced at higher S/C values. The increase in the water content in the feed favors the WGS reaction (Eq. (8)).

It is clear from Fig. 8 that the methane yield decreases precipitously as the temperature increases. However, at a fixed temperature and S/C ratio, the methane yield continues to decrease as the O/C ratio increases.

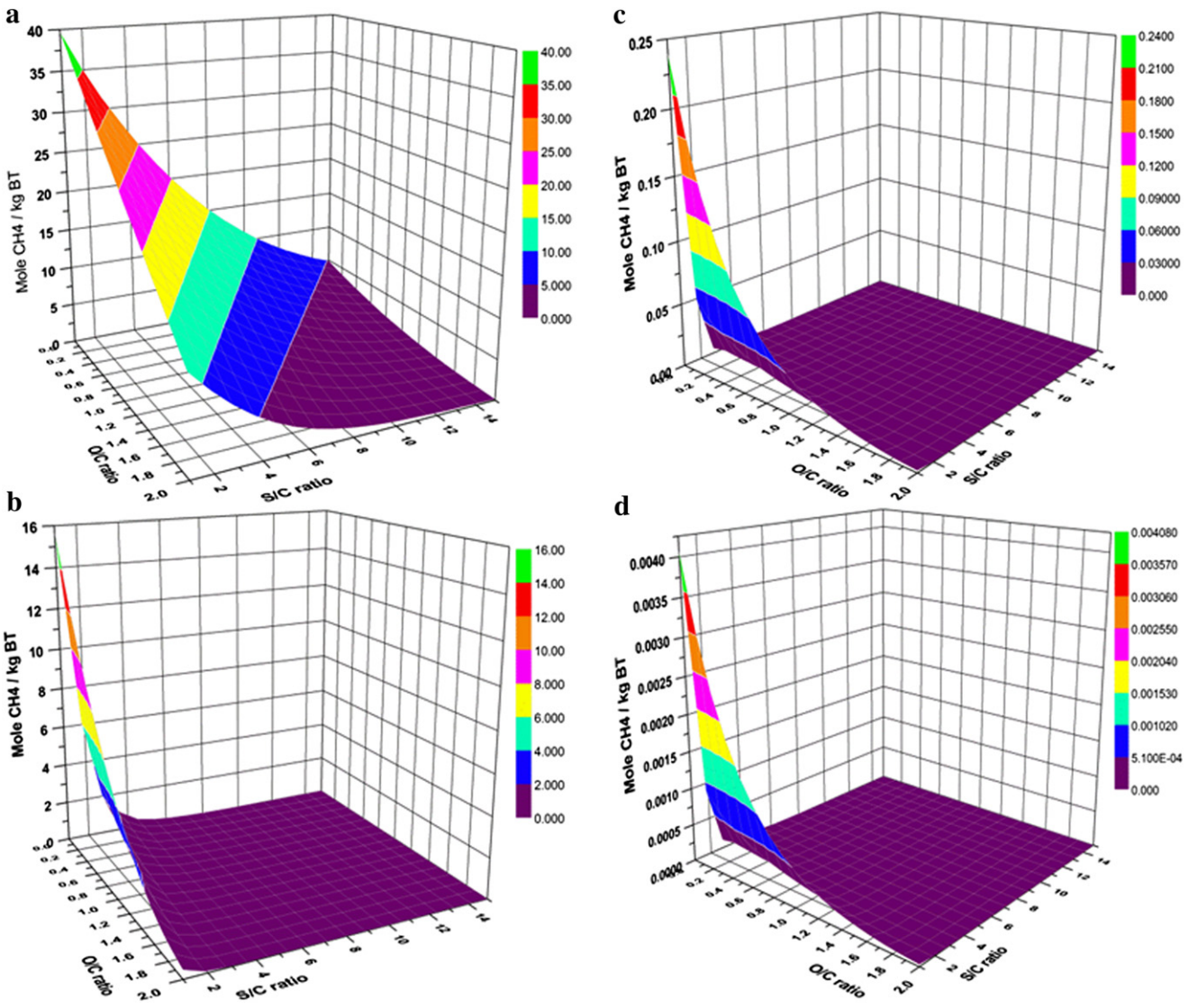

Fig. 8 – Moles of CH_4 produced per kg of BT in ATR reactor as function of S/C and O/C ratios at different temperatures and 1 atm: (a) 400 °C, (b) 600 °C, (c) 800 °C and (d) 1000 °C.

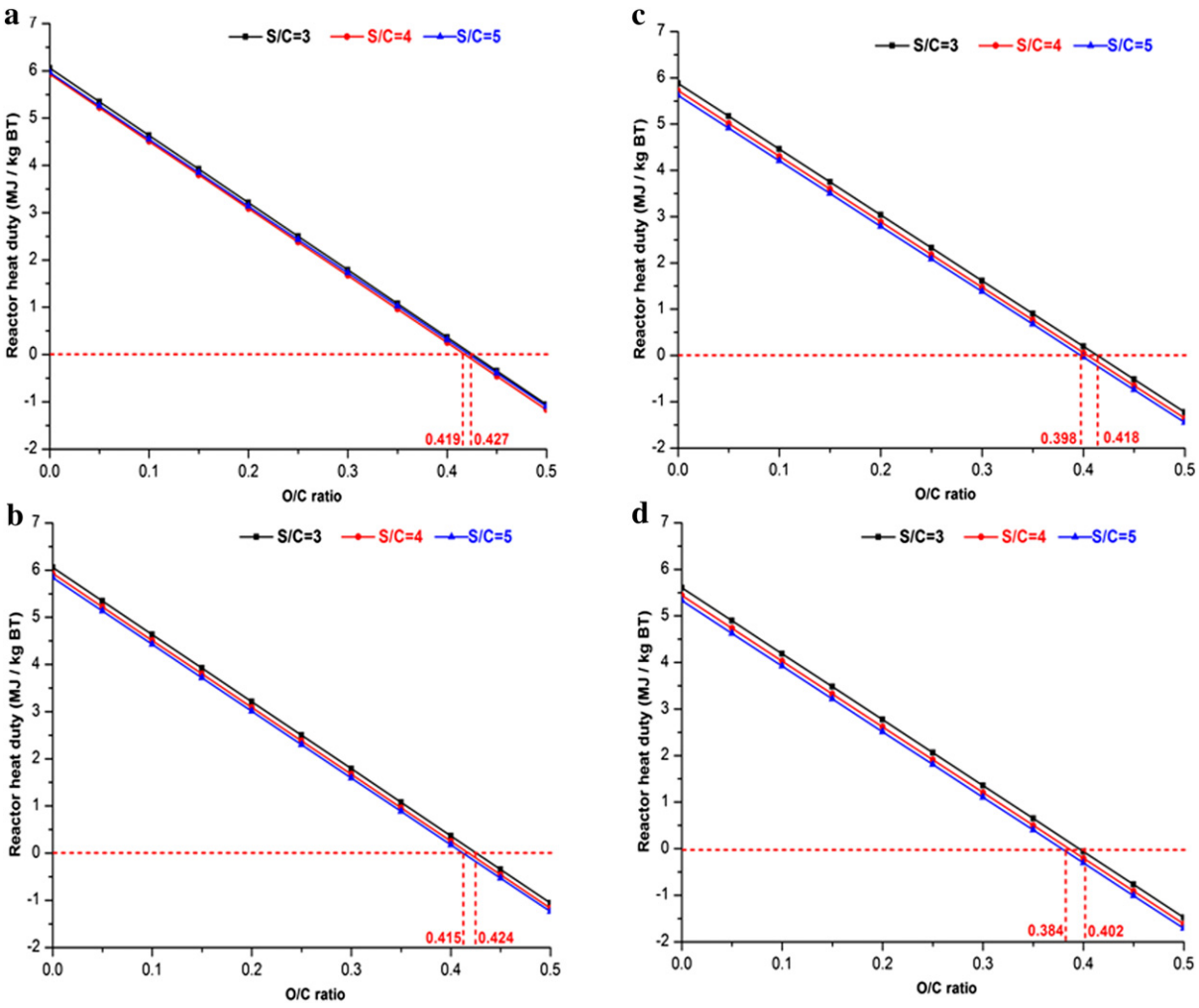

Fig. 9 – Reactor heat duty as a function of O/C and S/C ratios at 1 atm and different temperatures: (a) 600 °C, (b) 700 °C, (c) 800 °C and (d) 900 °C.

In conclusion, high hydrogen yield (green part in Fig. 6), moderate carbon monoxide yield (yellow part in Fig. 7), trace amounts of methane (purple part in Fig. 8) and no coke formation can be achieved simultaneously. Hydrogen production via ATR of BT can be optimized at temperatures of 600–800 °C, S/C ratios of 3–5, and O/C ratios of 0.0–0.45. (For interpretation of the color in these figures the reader is referred to the web version of this article.) ATR is an excellent method because of its ability to achieve a thermoneutral or slightly exothermic reaction by adjusting the feed ratios, which can reduce the need to heat the reactor [44]. Further optimum conditions for hydrogen production will be discussed in the thermoneutral condition discussion.

4.5. *Thermoneutral conditions*

In an autothermal steam reforming process, oxygen supplies the necessary heat via the oxidation reaction for endothermic steam reforming; therefore, increasing the O/C ratio decreases the external heat requirement. The operating temperature at which the external heat flow is equal to zero is also known as an adiabatic temperature. As a result, it is possible to operate the reformer with no external energy for cooling or heating, which makes it valuable from an energy consumption point of view [45].

The thermoneutral investigation is performed by considering BT, steam and oxygen as feeds entered into the reactor at the temperature of reactor.

Fig. 9 shows the variation in the heat duty with O/C ratios at different S/C ratios and temperatures. The O/C ratio has a very strong effect on the heat of reaction. The increase in O/C ratio can even transform the overall reaction from endothermic to exothermic. At 600 °C, O/C ratios of 0.419–0.427 are feasible to obtain thermoneutral conditions with the S/C values between 3 and 5, whereas at 900 °C, the O/C is 0.384–0.402. For all configurations considered, the thermoneutrality was obtained with an O/C ratio of 0.384–0.427.

The recommended conditions, which maximize hydrogen production while minimizing the methane and carbon monoxide contents and without forming coke at thermoneutral conditions, are S/C = 5, T = 600 °C and O/C = 0.422. Table 6 gives the synthesis gas composition at the optimum conditions of BT ATR reactor.

Table 6 – Characteristics of BT ATR reactor at optimum condition.

Reactor conditions				Synthesis gas composition % (dry basis)			
S/C	T (°C)	O/C	P (atm)	H_2	CO	CO_2	CH_4
5	600	0.422	1	70.10	2.92	26.91	0.07
Hydrogen productivity				150 mole/kg BT			

5. Conclusion

Thermodynamic equilibrium of BT steam and autothermal reforming was studied under atmospheric pressure via Gibbs free energy minimization, accounting for the possibility of coke formation. BT was considered as a mixture of triglycerides consisting of the three same fatty acid groups in their structure. The equilibrium compositions were calculated with the aid of the Aspen Plus™ software. Before the simulation could be started, triglycerides, main components of BT and non-databank compounds of Aspen Plus™, were added.

The study started with an expanded product set, approximately 30 by-products, to evaluate the thermodynamically possible products. Based on the thermodynamic calculation, the following conclusions can be drawn.

- Thermodynamically, CH_4 and C (graphite) are important products that coexist with H_2O, CO_2, CO and H_2, while the formation of by-products such as alkanes containing two or more carbon atoms, alkenes, acids and various alcohols are negligible.
- For SR system, the competition between carbon deposition and carbon elimination reactions makes the coke formation plot with non-monotone behavior. At a given temperature, an increase in the S/C lowered the amount of coke formed and for S/C ratios higher than 1, no coke can be formed at temperatures above 300 °C.
- The coke formation behavior in the case of ATR shows, for a given temperature, that coke formation is suppressed by the increase of the O/C ratio and/or the increase of the S/C ratio. Avoidance of coke formation is possible for S/C ratios higher than 1 and with temperatures above 300 °C.
- The optimum conditions for the SR of BT, determined for maximizing hydrogen production while minimizing the methane and carbon monoxide contents and coke formation, can be achieved at reforming temperatures between 700 °C and 900 °C and an S/C ratio of approximately 5. The optimal operation conditions for the SR of BT are proposed as $T = 700$ °C and an S/C ratio = 5. With these conditions, a hydrogen yield of 170 moles/kg BT and a CO concentration in the synthesis gas of 4.77%, with trace content of CH_4 (0.01%), can be obtained without the danger of carbon deposits.
- The most favorable conditions for hydrogen production from the ATR system are achieved with the temperatures, S/C ratios and O/C ratios of 600–800 °C, 3–5 and 0.0–0.45, respectively. Thermoneutral conditions under these conditions can be achieved with an O/C ratio of 0.384–0.427. The recommended conditions, which maximize hydrogen production while minimizing the methane and carbon monoxide contents and without forming coke at thermoneutral conditions, are $S/C = 5$, $T = 600$ °C and $O/C = 0.422$. Under these conditions, 150 moles H_2/kg BT can be produced with only 2.92% CO and 0.07% CH_4 in the synthesis gas.

Finally, creating an energetic application for tallow avoids its tendency to be utilized as a food additive, with the associated risks to human health. Moreover, because tallow is derived from animal by-products, which have little to no value, it avoids some of the food vs. fuel debate. Hydrogen production via tallow reforming is thermodynamically feasible, and further investigation through experimental work would be greatly beneficial for understanding this process. This work provides a full thermodynamic investigation that is useful to guide the study for the high purity hydrogen production via beef tallow reforming for fuel cell application.

REFERENCES

[1] Marbán G, Valdés-Solís T. Towards the hydrogen economy? Int J Hydrogen Energy 2007;32:1625–37.
[2] Crnkovic PM, Koch C, Ávila I, Mortari DA, Cordoba AM, dos Santos AM. Determination of the activation energies of beef tallow and crude glycerin combustion using thermogravimetry. Biomass Bioenergy 2012;44:8–16.
[3] Almansoori A, Shah N. Design and operation of a future hydrogen supply chain: multi-period model. Int J Hydrogen Energy 2009;34:7883–97.
[4] Wang X, Jin B. Process optimization of biological hydrogen production from molasses by a newly isolated *Clostridium butyricum* W5. J Biosci Bioeng 2009;107:138–44.
[5] Adamson K. Hydrogen from renewable resources – the hundred year commitment. Energy Policy 2004;32:1231–42.
[6] Kotay S, Das D. Biohydrogen as a renewable energy resource – prospects and potentials. Int J Hydrogen Energy 2008;33:258–63.
[7] Ramani K, John Kennedy L, Ramakrishnan M, Sekaran G. Purification, characterization and application of acidic lipase from Pseudomonas gessardii using beef tallow as a substrate for fats and oil hydrolysis. Process Biochem 2010;45:1683–91.
[8] Dale N, Howes P, Miller R, Watson P. Advice on the economic and environmental impacts of government support for biodiesel production from tallow. Report to the Department of Transport, Copyright AEA Technology plc; 2008.
[9] Deferne J, Pate DW. Hemp seed oil: a source of valuable essential fatty acids. J Int Hemp Assoc 1996;3:4–7.
[10] Carvalho IS, Miranda I, Pereira H. Evaluation of oil composition of some crops suitable for human nutrition. Ind Crop Prod 2006;24:75–8.
[11] Marquevich M, Medina F, Montané D. Hydrogen production via steam reforming of sunflower oil over Ni/Al catalysts from hydrotalcite materials. Catal Commun 2001;2:119–24.
[12] Dupont V, Ross AB, Hanley I, Twigg MV. Unmixed steam reforming of methane and sunflower oil: a single-reactor process for image-rich gas. Int J Hydrogen Energy 2007;32:67–79.
[13] Yenumala SR, Maity SK. Reforming of vegetable oil for production of hydrogen: a thermodynamic analysis. Int J Hydrogen Energy 2011;36:11666–75.
[14] Pumps World. Turning tallow oil into biodiesel fuel, www.worldpumps.com; 2010.
[15] da Cunha ME, Krause LC, Moraes MSA, Faccini CS, Jacques RA, Almeida SR, et al. Beef tallow biodiesel produced in a pilot scale. Fuel Process Technol 2009;90:570–5.

[16] Öner C, Altun Ş. Biodiesel production from inedible animal tallow and an experimental investigation of its use as alternative fuel in a direct injection diesel engine. Appl Energy 2009;86:2114–20.
[17] Bhatti HN, Hanif MA, Qasim M, Rehman A. Biodiesel production from waste tallow. Fuel 2008;87:2961–6.
[18] Teixeira LSG, Couto MB, Souza GS, Filho MA, Assis JCR, Guimarães PRB, et al. Characterization of beef tallow biodiesel and their mixtures with soybean biodiesel and mineral diesel fuel. Biomass Bioenergy 2010;34:438–41.
[19] Evans L, Okamura S, Poll J, Barke N. Evaluation of opportunities for converting indigenous UK wastes to fuels and energy. AEA Energy Environ 2009.
[20] USDA, United States Department of Agriculture, www.usda.gov; 2012.
[21] Eurostat, Statistical Office of the European Union, epp.eurostat.ec.europa.eu; 2012.
[22] Nelson RG, Schrock MD. Energetic and economic feasibility associated with the production, processing, and conversion of beef tallow to a substitute diesel fuel. Biomass Bioenergy 2006;30:584–91.
[23] Teixeira LSG, Assis JCR, Mendonça DR, Santos ITV, Guimarães PRB, Pontes LAM. Comparison between conventional and ultrasonic preparation of beef tallow biodiesel. Fuel Process Technol 2009;90:1164–6.
[24] Shi B, O'Brien RJ, Bao S, Davis BH. Mechanism of the isomerization of 1-alkene during iron-catalyzed Fischer–Tropsch synthesis. J Catal 2001;199:202–8.
[25] National Research Council. Fat content and composition of animal products. Washington, D.C: Printing and Publishing Office, National Academy of Science, ISBN 0-309-02440-4; 1976.
[26] Aspen Plus™. Physical property methods and models software version. USA: Burlington MA: Aspen Technology Inc; 1988.
[27] Morad NA, Kamal AAM, Panau F, Yew TW. Liquid specific heat capacity estimation for fatty acids, triacylglycerols, and vegetable oils based on their fatty acid composition. J Am Oil Chem Soc 2000;77:1001–5.
[28] Goodrum JW, Deller DP. Rapid thermogravimetric measurements of boiling points and vapor pressure of saturated medium- and long-chain triglycerides. Bioresour Technol 2002;84:75–80.
[29] da Silva AL, Müller IL. Hydrogen production by sorption enhanced steam reforming of oxygenated hydrocarbons (ethanol, glycerol, n-butanol and methanol): thermodynamic modeling. Int J Hydrogen Energy 2011;36:2057–75.
[30] Lwin Y, Daud WRW, Mohamad AB, Yaakob Z. Hydrogen production from steam–methanol reforming: thermodynamic analysis. Int J Hydrogen Energy 2000;25:47–53.
[31] Perna A. Hydrogen from ethanol: theoretical optimization of a PEMFC system integrated with a steam reforming processor. Int J Hydrogen Energy 2007;32:1811–9.
[32] Nahar GA, Madhani SY. Thermodynamic of hydrogen production by the steam reforming of butanol: analysis of inorganic gases and light hydrocarbons. Int J Hydrogen Energy 2010;35:98–109.
[33] Ahmed S, Krumpelt M. Hydrogen from hydrocarbon fuels for fuel cells. Int J Hydrogen Energy 2001;26:291–301.
[34] Yoon HC, Erickson PA. Hydrogen from coal-derived methanol via autothermal reforming processes. Int J Hydrogen Energy 2008;33:57–63.
[35] Palmeri N, Chiodo V, Freni S, Frusteri F, Bart JCJ, Cavallaro S. Hydrogen from oxygenated solvents by steam reforming on Ni/Al2O3 catalyst. Int J Hydrogen Energy 2008;33:6627–34.
[36] Wu C, Liu RH. Carbon deposition behavior in steam reforming of bio-oil model compound for hydrogen production. Int J Hydrogen Energy 2010;35:7386–98.
[37] Chen WH, Lin MR, Lu JJ, Chao Y, Leu TS. Thermodynamic analysis of hydrogen production from methane via autothermal reforming and partial oxidation followed by water gas shift reaction. Int J Hydrogen Energy 2010;35:11787–97.
[38] Ávila-Neto CN, Dantas SC, Silva FA, Franco TV, Romanielo LL, Hori CE, et al. Hydrogen production from methane reforming: thermodynamic assessment and autothermal reactor design. J Nat Gas Sci Eng 2009;1:205–15.
[39] Liu Z, Mao Z, Xu J, Hess-Mohr N, Schmidt VM. Operation conditions optimization of hydrogen production by propane autothermal reforming for PEMFC application. Chinese J Chem Eng 2006;14:259–65.
[40] Zeng G, Tian Y, Li Y. Thermodynamic analysis of hydrogen production for fuel cell via oxidative steam reforming of propane. Int J Hydrogen Energy 2010;35:6726–37.
[41] Graschinsky C, Giunta P, Amadeo N, Laborde M. Thermodynamic analysis of hydrogen production by autothermal reforming of ethanol. Int J Hydrogen Energy 2012;37:10118–24.
[42] Rabenstein G, Hacker V. Hydrogen for fuel cells from ethanol by steam-reforming, partial-oxidation and combined auto-thermal reforming: a thermodynamic analysis. J Power Sources 2008;185:1293–304.
[43] Authayanun S, Arpornwichanop A, Paengjuntuek W, Assabumrungrat S. Thermodynamic study of hydrogen production from crude glycerol autothermal reforming for fuel cell applications. Int J Hydrogen Energy 2010;35:6617–23.
[44] Wang H, Wang X, Li M, Li S, Wang S, Ma X. Thermodynamic analysis of hydrogen production from glycerol autothermal reforming. Int J Hydrogen Energy 2009;34:5683–90.
[45] Kale GR, Kulkarni BD. Thermodynamic analysis of dry autothermal reforming of glycerol. Fuel Process Technol 2010;91:520–30.